Influence of collisional dephasing processes on superfluorescence

Jeffery J. Maki, Michelle S. Malcuit, Michael G. Raymer,* and Robert W. Boyd
Institute of Optics, University of Rochester, Rochester, New York 14627

Peter D. Drummond
Department of Physics, University of Queensland, Brisbane, Australia
(Received 23 January 1989; revised manuscript received 6 July 1989)

We present a quantum-mechanical treatment of the influence of collisional dephasing processes on the statistical properties of superfluorescence (SF). The theory, which treats nonlinear propagation effects as well as quantum noise, shows how the nature of the cooperative emission process changes from that of SF to that of amplified spontaneous emission as the collisional dephasing rate is varied. The predictions of how the SF delay time varies with the collisional dephasing rate are in good agreement with the results of a recent experiment [M. S. Malcuit, J. J. Maki, D. J. Simkin, and R. W. Boyd, Phys. Rev. Lett. **59**, 1189 (1987)].

I. INTRODUCTION

Superfluorescence (SF) is the cooperative radiative decay of a collection of initially inverted atoms.[1-7] The simplest theories of SF often ignore many of the complications that occur in actual experimental studies, such as the presence of line-broadening mechanisms and the effects of propagation. However, these effects can have a profound influence on the character of SF. For instance, a recent experimental study[8] performed in part by several of the present authors showed that the character of the cooperative emission changes from that of SF to that of amplified spontaneous emission[9-12] (ASE) as the collisional dephasing rate is increased. The results of this experiment agreed well with the predictions of a semiclassical theory developed by the authors. In the present paper we present a quantum-mechanical theory of cooperative emission from a collisionally broadened medium and use the predictions of this new calculation to interpret the results of the aforementioned experiment. This new theory is based on a fully quantum-mechanical derivation, where a correspondence between operators and c numbers is made using quasiprobability methods.[13-20] We believe that this quantum-mechanical theory can provide a more firm theoretical understanding of the manner in which the character of the cooperative emission process is modified by the presence of homogeneous dephasing processes.

Figure 1 shows the various regimes in which cooperative emission can occur. The axes give the total number N of interacting atoms and the intensity gain αL associated with a single pass through the interaction region of length L. The gain axis can alternatively be thought of as a normalized dephasing time, since (as pointed out by Friedberg and Hartmann[21])

$$\alpha L = \frac{2T_2}{\tau_r} , \tag{1}$$

where T_2 is the dipole-dephasing time. The "cooperative lifetime,"[22]

$$\tau_r = \frac{8\pi A}{3\lambda^2}\frac{T_1}{N} , \tag{2}$$

gives the characteristic time scale of SF, and is expressed in terms of the cross-sectional area A of the excited region, the transition wavelength λ, and the inverse of the Einstein A coefficient T_1. In the limit of negligible dephasing, the SF process occurs in the form of a short pulse whose duration is of the order τ_r and which is de-

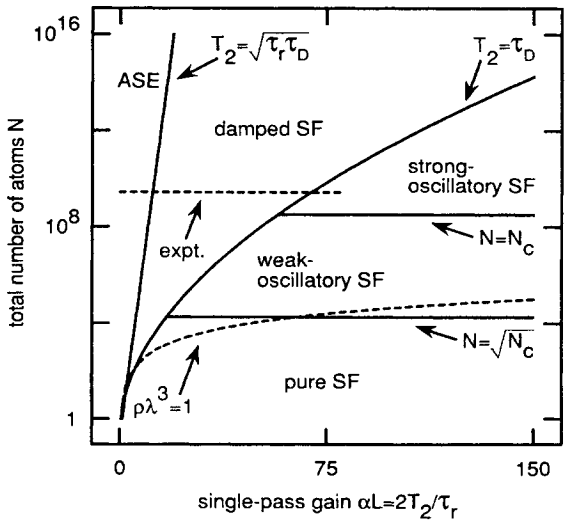

FIG. 1. Regimes of N-atom cooperative spontaneous emission. For $T_2 < (\tau_r\tau_D)^{1/2}$ amplified spontaneous emission (ASE) occurs, whereas for $T_2 > \tau_D$ superfluorescence (SF) occurs, with damped SF occurring for intermediate values of T_2. Strong-oscillatory, weak-oscillatory, and pure SF occur depending on the value of N compared to the cooperation number N_c. The case $N_c = 3\times 10^8$ is shown. The dashed line labeled $\rho\lambda^3 = 1$ shows how N and αL are related for the case in which the density is held fixed at $\rho = \lambda^{-3}$, for a Fresnel number $F = 1$, and for $T_2 = 2T_1$. The other dashed line shows the range of parameters studied in the experiment and theory.

layed with respect to the excitation by a delay time τ_D. The delay time is much larger than τ_r and has been shown by Polder, Schurrmans and Vrehen[23] to be estimated by

$$\tau_D = \tau_r[\tfrac{1}{4}\ln(2\pi N)]^2 . \quad (3)$$

Figure 1 is divided into several different regions, each of which is given a name that the present authors find useful in describing the nature of the emission process under the indicated conditions. We stress that not all authors use these names in exactly the same sense in which we use them. The primary division of Fig. 1 is based on the relative importance of dephasing processes and divides the parameter space into three regions labeled ASE, damped SF, and SF.[2] These regions are separated by the curves labeled $T_2=(\tau_r\tau_D)^{1/2}$ and $T_2=\tau_D$. The region to the right of the second curve (labeled SF) is the region in which $T_2>\tau_D$ (or $\alpha L>[ln(2\pi N)]^2/8$), that is, the region in which on average no collision occurs during the SF buildup time. In this region the effects of collisional dephasing are negligibly small, allowing the cooperative emission process to occur with the buildup of a macroscopic dipole moment. Schuurmans and Polder have shown that for $T_2<(\tau_r\tau_D)^{1/2}$ [or $\alpha L<\ln(2\pi N)/2$] the amount of dephasing will be sufficient to prevent the occurrence of cooperative emission.[2,24,25] In this limit no macroscopic dipole moment can build up and the atoms simply respond to the instantaneous value of the radiation field. The region to the left of the curve for $T_2=(\tau_r\tau_D)^{1/2}$ is hence labeled ASE. The region between these two curves in which collisional dephasing effects can play some role in inhibiting the cooperative radiative decay is labeled damped SF.

The region of Fig. 1 labeled SF is further divided into three regions labeled pure SF, weak-oscillatory SF, and strong-oscillatory SF by the curves labeled $N=N_c$ and $N=N_c^{1/2}$. Here N_c denotes the Arecchi-Courtens[26] cooperation number

$$N_c=\frac{8\pi cT_1A}{3\lambda^2L} , \quad (4)$$

which is a measure of the maximum number of atoms that can emit cooperatively. We have plotted these lines for the particular value $N_c=3\times10^8$, which is appropriate for the conditions of our experimental study using the material system[27] $KCl:O_2^-$, namely, $T_1=80$ ns, $\lambda=629$ nm, $L=0.7$ cm, and a Fresnel number ($F=A/\lambda L$) equal to unity. Bonifacio and Lugiato[28] have shown that propagation effects become important when N significantly exceeds N_c, leading to strong temporal ringing in the SF output due to reabsorption of the emitted radiation. More recently, Gross and Haroche[3,29] have shown that the more restrictive condition $N<N_c^{1/2}$ must be met in order for pure SF to occur, in which propagation effects are presumed not to be important.

We have also plotted in the figure the dashed line labeled $\rho\lambda^3=1$, where ρ denotes the number density of excited atoms ($\rho=N/AL$). The region below this line can be reached only through the use of a number density greater than λ^{-3}. For densities this large, near-field dipole-dipole interactions become significant,[30,31] and the effects of such interactions have not been included in previous (or the present) treatments of extended sample SF. The functional form of the dashed line is $\alpha L=(3/4\pi)(T_2/T_1)(N/F)^{1/2}$. This form is obtained through the use of Eqs. (1) and (2) and the assumption that $\rho\lambda^3=1$. The dashed line as shown is plotted for the values $F=1$ and $T_2/T_1=2$. We performed our experimental study of the transition from SF to ASE using a sample containing a total number of excited atoms equal to 3×10^9, well outside the region where near-field dipole-dipole interactions are important.

II. EXPERIMENT

Our experiment entailed studying the nature of the cooperative emission process for several different values of the temperature of a $KCl:O_2^-$ sample and hence for different values of the dipole dephasing time T_2. Some of the experimental results of this study are shown in Fig. 2. Here for six different values of the temperature of the crystal, we show typical experimental realizations of the time evolution of the intensity of the cooperative emission. As the temperature of the crystal is increased, thereby increasing the dipole dephasing rate,[32] the nature of the emission is seen to evolve gradually from that of SF to that of ASE. We have quantified these results by determining how the delay time of the emission depends

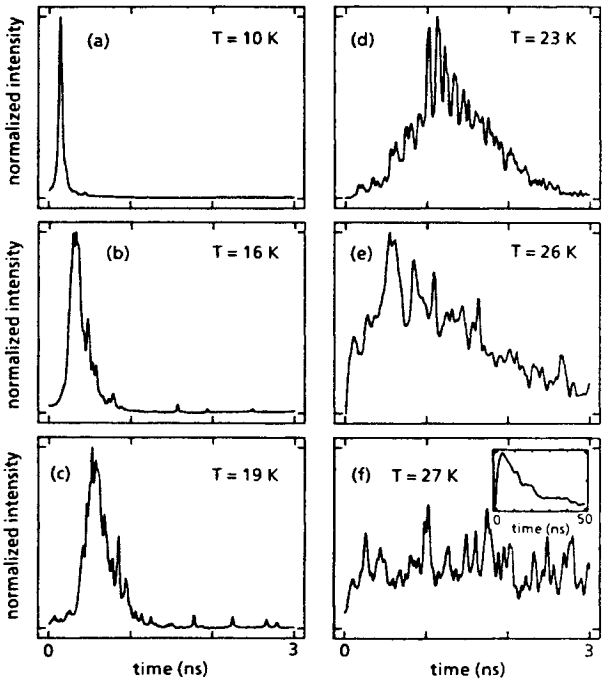

FIG. 2. Typical experimental realizations of the temporal evolution of the emission from $KCl:O_2^-$ for several different temperatures. At the lowest temperature, the emission is characteristic of SF, whereas at the highest temperature the emission is characteristic of ASE. The inset to case (f) shows the evolution of the emission on a longer time scale.

on the dipole dephasing time, as shown in Fig. 3. We have used two different ways of characterizing the delay time of the emission. One method involves estimating the delay time associated with each experimental realization of the emission, where in the present case the delay time is taken to be the time required to reach the peak of the emitted intensity. For the data collected at higher temperatures, where the time evolution is quite noisy, we first fit a smooth curve through the data before determining its peak. For each value of the temperature, the solid squares shown in Fig. 3(a) give the average value of the delay time according to this definition. The analysis of delay-time statistics could instead have been done using an energy passage time, defined to be the time required for a certain amount of energy to be emitted. The energy passage time has the desirable property that it is less sensitive to fluctuations for cases where the emission is quite noisy.[33] Our other method of analyzing the data entails first determining the ensemble average of the time evolution of the intensity and then estimating the time delay of this ensemble-average intensity. These results are shown by the solid squares in Fig. 3(b). This second method is of interest because certain theoretical treatments of SF (see below) can predict the time evolution of the ensemble-averaged intensity but cannot make predictions regarding even the statistical behavior of individual realizations of the emission process. Note that these two different estimates of the time delay differ significantly in the transition region between that of SF and ASE. The reason for this difference is that each realization contains roughly the same energy. Consequently, realizations with shorter-than-average delay times preferentially have higher-than-average intensities at small times, and hence the ensemble-averaged intensity for small times is disproportionately weighted by such realizations.

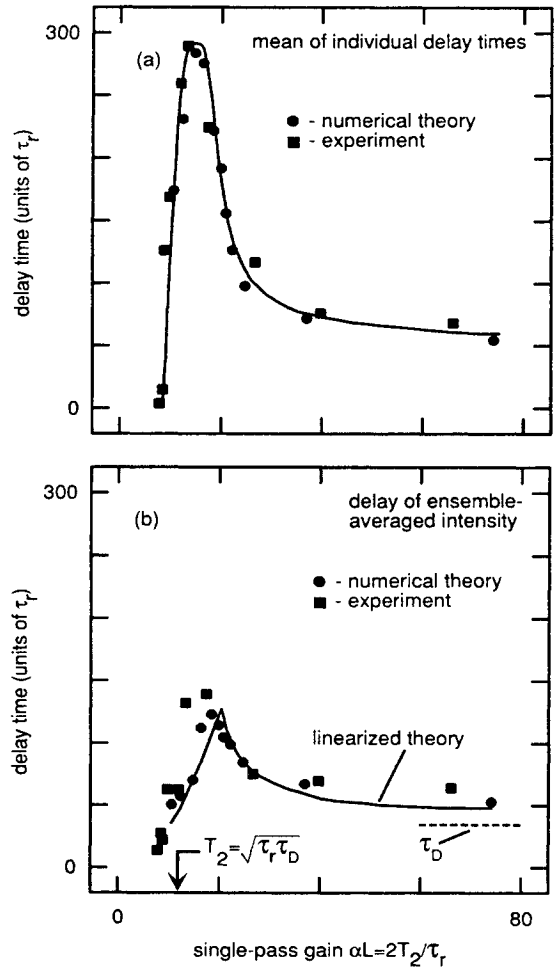

FIG. 3. Delay times as functions of the single-pass gain. The squares are the values found from the experiment, while the circles are the values found from the theory. (a) gives the mean value of the individual delay times, while (b) gives the delay time of the ensemble-averaged intensity. The solid line in (a) is an aid to the eye. The solid line in (b) gives the value of the delay times found using the linearized theory, Eq. (15). The arrow marked $T_2=(\tau_r\tau_D)^{1/2}$ gives the value of the gain corresponding to the Schuurmans-Polder criterion for the transition to ASE and the dashed line gives the theoretical value [Eq. (3)] of the delay time in the limit of no dipole dephasing.

III. QUANTUM THEORY OF SF

In our previous paper,[8] we interpreted our experimental results by means of a semiclassical model that included the effects of propagation and of homogeneous dephasing. We used a semiclassical approach because the only available quantum-mechanical treatments[24,34] of SF that included the effects of propagation and of homogeneous dephasing assumed the condition of constant inversion and hence were valid only for the initiation period of the emission. Quantum-mechanical theories that can describe the temporal evolution of the emission beyond the initiation regime exist, but treat the case of inhomogeneous broadening.[2,25,35] In the present paper, we reanalyze our results in terms of the fully quantum-mechanical theory developed originally by Haken[15] and Louisell.[16] This theory was later generalized[17–19] to a positive distribution representation, in order to describe the quantum-statistical properties of optical bistability. The details of the derivation leading to the equations of motion needed here are given in Ref. 36. In applying this formalism to the present problem, we assume that initially the medium is totally inverted. Through the use of the positive P representation,[17,18] it is found that the operator equations describing the coupled atom-field system can be converted to (c-number) Itô stochastic differential equations.[37] To leading order in a $1/N$ expansion for N atoms, these equations are

$$\frac{\partial}{\partial t}\alpha_s^- = -\sum_{s'} i\Delta_{ss'}\alpha_{s'}^- + \tilde{g}J_s^- \ , \tag{5a}$$

$$\frac{\partial}{\partial t}J_s^- = -\gamma_2 J_s^- + \tilde{g}\alpha_s^- D_s + \Gamma_s^{J^-} \ , \tag{5b}$$

$$\frac{\partial}{\partial t}D_s = -\gamma_1(D_s+N_s) - 2\tilde{g}[(J_s^-)^*\alpha_s^- + J_s^-(\alpha_s^-)^*] + \Gamma_s^D \ , \tag{5c}$$

where α_s^- is the electric field amplitude, and J_s^- and D_s are the atomic polarization and inversion, respectively, at

the position z_s. The correspondence between c numbers and operators is as follows:

$$\alpha_s^- \leftrightarrow (2M+1)^{-1/2} \sum_{m=-M}^{M} \hat{a}_m \exp(im\Delta k z_s + i\omega_0 t) , \quad (6a)$$

$$J_s^- \leftrightarrow \sum_{\mu} \hat{\sigma}_{\mu}^- \exp(-i\mathbf{k}_0 \cdot \mathbf{r}_{\mu} + i\omega_0 t) , \quad (6b)$$

$$D_s \leftrightarrow \sum_{\mu} \hat{\sigma}_{\mu}^z , \quad (6c)$$

where ω_0 is the atomic-transition frequency. The field operator $\hat{a}_m$ is the lowering operator for the field mode having wave vector $k_m = k_0 + m\Delta k$ along the axis of the interaction region, where $k_0 = \omega_0/c$ and $\Delta k = 2\pi/L$. The Pauli operators σ_{μ}^- and $\hat{\sigma}_{\mu}^z$ describe the atom located at position $\mathbf{r}_{\mu}$. The summation over μ in Eqs. (6b) and (6c) is to be performed over the total number N_s of atoms within the volume element (or slice) of cross-sectional area A and thickness $\Delta z = L/(2M+1)$ located at $z_s = s\Delta z$, where s is an integer that ranges in value from $-M$ to M. Here $2M+1$ is the number of volume elements into which the sample has been divided. The atom-field coupling constant $\tilde{g}$ for a given volume element is related to the single-mode atom-field coupling constant $g = d(2\pi\omega_0/\hbar V)^{1/2}$ by $\tilde{g} = (2M+1)^{1/2} g$, where d is the atomic dipole transition moment and $V = AL$ is the total volume of the interaction region. The atomic damping and dephasing rates are given by $\gamma_1 = 1/T_1$ and $\gamma_2 = 1/T_2$, respectively.

The theory developed by Drummond and Walls[18] to treat optical bistability is a mean-field model. We have generalized their theory to include one-dimensional propagation effects[20] by the inclusion of the term $\Delta_{ss'}$ in Eq. (5a). This term is given by

$$\Delta_{ss'} = \sum_{m=-M}^{M} \frac{mc\Delta k}{2M+1} \exp[im\Delta k(z_s - z_{s'})] , \quad (7)$$

and describes how the field in slice s is related to the field in slice s'. The one-dimensional model is fairly accurate when the Fresnel number of the medium is of the order of unity,[38] as in our experiment.

In general, the stochastic source terms in Eqs. (5) can give rise to nonclassical statistical behavior. However, we approximate these noise terms by

$$\Gamma_s^J = [\gamma_p(D_s + N_s)/2]^{1/2}(\xi_{1,s} + i\xi_{2,s}) , \quad (8a)$$

$$\Gamma_s^D = [2\gamma_1(D_s + N_s)]^{1/2}\xi_{3,s} , \quad (8b)$$

where $\gamma_p = \gamma_2 - \gamma_1/2$ and where the ξ_i are real, Gaussian, random variables of zero mean correlated according to

$$\langle \xi_{i,s}(t)\xi_{j,s'}(t') \rangle = \delta_{ij}\delta_{ss'}\delta(t-t') , \quad (9)$$

where i and j equal 1, 2, and 3. In writing Eqs. (8) we have included only the inversion-dependent contributions to the stochastic sources, which is appropriate since they are the dominant contributions for the case of an initially inverted medium.[39] The terms included here, therefore, generate only classical statistical noise, in the sense that the field distributions always have a Glauber-Sudarshan P representation that is positive. This approximation precludes the study of nonclassical states of the field, which are not of interest here.

Equations (5) can be rewritten in the form usually used in theories of cooperative emission by rescaling the quantities and by transforming the equations to a description involving a continuous spatial variable x that varies between 0 and 1. Under the assumption of no interaction between the counter-propagating waves within the sample, the stochastic equations for the description of the emission traveling in the positive x direction at retarded time $\tau = (t - xL/c)/\tau_r$ are

$$\frac{\partial}{\partial x} e(x,\tau) = p(x,\tau) , \quad (10a)$$

$$\frac{\partial}{\partial \tau} p(x,\tau) = -\tilde{\gamma}_2 p(x,\tau) + e(x,\tau)n(x,\tau) + \Gamma^p(x,\tau) , \quad (10b)$$

$$\frac{\partial}{\partial \tau} n(x,\tau) = -\tilde{\gamma}_1[n(x,\tau)+1] - 2[p^*(x,\tau)e(x,\tau) + p(x,\tau)e^*(x,\tau)] + \Gamma^n(x,\tau) , \quad (10c)$$

where the following correspondence between discrete and continuous variables exists: $e(x,\tau) \leftrightarrow \tau_r \tilde{g} \alpha_s^-(t)$, $p(x,\tau) \leftrightarrow J_s^-(t)/N_s$, and $n(x,\tau) \leftrightarrow D_s(t)/N_s$. The stochastic source terms are now

$$\Gamma^p(x,\tau) = \{\tilde{\gamma}_p[n(x,\tau)+1]/2N\}^{1/2} \times [\xi_1(x,\tau) + i\xi_2(x,\tau)] , \quad (11a)$$

$$\Gamma^n(x,\tau) = \{2\tilde{\gamma}_1[n(x,\tau)+1]/N\}^{1/2}\xi_3(x,\tau) , \quad (11b)$$

where the ξ_i are Gaussian random variables of zero mean with the correlation

$$\langle \xi_i(x,\tau)\xi_j(x',\tau') \rangle = \delta_{ij}\delta(x-x')\delta(\tau-\tau') , \quad (12)$$

where i and j equal 1, 2, and 3. The dimensionless decay rates are given by $\tilde{\gamma}_2 = \tau_r\gamma_2$, $\tilde{\gamma}_1 = \tau_r\gamma_1$, and $\tilde{\gamma}_p = \tilde{\gamma}_2 - \tilde{\gamma}_1/2$. We note that Eqs. (10) are equivalent to the semiclassical Maxwell-Bloch[40] equations except for the added stochastic source terms Γ^p and Γ^n.

We solve Eqs. (10) numerically for $N = 3\times 10^9$, in agreement with the experimental conditions of Ref. 8. We assume that no external field impinges on the sample at $x = 0$, except for an initial excitation pulse that travels through the sample in the positive x direction (swept gain). Because we have omitted the nonclassical noise terms, Eqs. (10) constitute five independent real equations, in our case. In the full quantum-statistical theory five independent complex equations would replace Eqs. (10). The exact quasiprobability distributions are highly singular for inverted atoms. However, in the present $(1/N)$ expansion, an approximate Gaussian distribution reproduces the moments of the quantum fluctuations to the required order in the expansion. In fact, these distributions also occur in the solution for an optically pumped medium when the present truncation approximation is

used.[36] For each slice, the initial correlations in the polarization and inversion are

$$\langle J_s^- J_{s'}^+ \rangle = N_s \delta_{ss'} , \tag{13a}$$

$$\langle D_s D_{s'} \rangle = 0 . \tag{13b}$$

Hence, in the continuum limit, the initial polarization $p(x,0)$ in retarded time is taken to be a random field given by[38]

$$p(x,0) = (2N)^{-1/2}[\xi_1(x) + i\xi_2(x)] , \tag{14}$$

where $\langle \xi_i(x)\xi_j(x') \rangle = \delta_{ij}\delta(x-x')$. Note that the random variable found by averaging $p(x,0)$ over a spatial slice has a variance that corresponds, within the Bloch-sphere formalism, to an rms tipping angle of $2/N_s^{1/2}$. The initial values of the variables for the inversion and the electric field are taken to have the deterministic values $e(x,0)=0$ and $n(x,0)=1$. Note that since the positive P representation assumes the case of normally ordered operators, the quantum uncertainty has shown up only in the polarization.

IV. RESULTS

The equations were solved numerically by using an Euler method (see the Appendix) appropriate for solving stochastic differential equations. Some of the results of these numerical simulations are given in Fig. 4. The three columns labeled "single realization" show particular realizations of this stochastic process for various values of the gain. The rows correspond to four different values of gain. For high gain [Fig. 4(a)] the emission is characteristic of SF and for low gain [Fig. 4(d)] the temporal evolution of the intensity is very noisy, a characteristic of ASE. Note that the qualitative character of the emission evolves gradually from that of SF to that of ASE as the single-pass gain is gradually decreased. For example, as we decrease the gain, the temporal ringing of SF is diminished and replaced with a pulse breakup phenomenon, where the first pulse is not necessarily the highest pulse. To characterize the stochastic nature of the emission process we have calculated 30 realizations of the temporal evolution of the emission for each value of the gain. For each value of the gain, we determine the average value of the delay time using the same method (described above) used in analyzing our experimental results to determine the mean of the individual delay times. The solid circles in Fig. 3(a) show these theoretical predictions. The agreement between the theory and experiment is quite good.

We note that a direct identification of experimental trajectories with quantum-stochastic trajectories is possible here because the photon numbers are extremely large. Quantum-stochastic averages can in general be identified with overall moments of the experimental data. In the

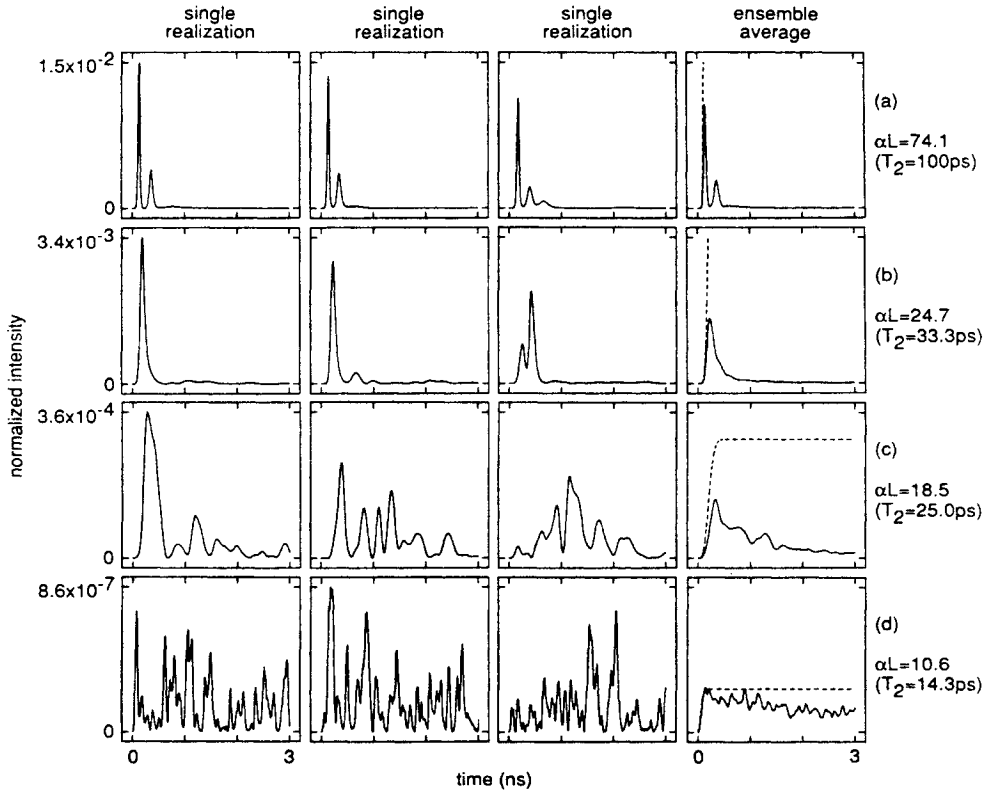

FIG. 4. Theoretical plots of the temporal evolution of the N-atom cooperative spontaneous emission. The plots labeled "single realization" give particular realizations of the emission for the given value of the single-pass gain. For the plots labeled "ensemble average," the solid curves give an estimate of this quantity based on averaging 30 realizations of Eqs. (10), while the dashed lines are plots of Eq. (15).

present case the variance caused by shot-noise effects at the detectors is relatively small. In addition, the removal of nonclassical noise from the simulations implies that only classical phase-space trajectories are available. For these reasons, the identification of stochastic and experimental moments implies that we can regard each stochastic trajectory as representing a typical, experimentally observable result.

The results of the numerical solution of Eqs. (10) have also been used to find the ensemble-averaged intensity. The curves drawn with a solid line in the fourth column of Fig. 4 labeled "ensemble average" show estimates of the ensemble-averaged intensity based on these 30 realizations of the emission for each value of the gain. We then calculate the delay time of these ensemble-averaged intensities. The solid circles of Fig. 3(b) show these theoretical predictions of the delay time of the ensemble-averaged intensity. The agreement between these theoretical predictions and the results of the experiment is again quite good.

It is useful to compare the results of our numerical calculation of the ensemble-averaged intensity to those of the approximate, analytic theory sometimes used to describe the initiation of SF. During the early stages of the cooperative emission process, the population inverse is essentially constant and equal to its initial value of unity [i.e., $n(x,\tau)=1$]. Under these conditions Eqs. (10a) and (10b) become linear and can be solved analytically to obtain the following expression for the ensemble-averaged intensity (normalized by $N\hbar\omega/A\tau_r$):

$$\langle I(\tau)\rangle=\frac{1}{N}\left[e^{-2\tilde{\gamma}_2\tau}[I_0^2(2\tau^{1/2})-I_1^2(2\tau^{1/2})]+2\tilde{\gamma}_p\int_0^{\tau}d\tau' e^{-2\tilde{\gamma}_2\tau'}[I_0^2(2\tau'^{1/2})-I_1^2(2\tau'^{1/2})]\right] . \tag{15}$$

Here I_0 and I_1 are the zeroth-order and first-order modified Bessel functions, respectively. This expression is identical to that relevant to stimulated Raman scattering and can be derived by methods identical to those described by Raymer and Mostowski.[41] Note that this expression is also that given by Haake *et al.* for the ensemble-averaged intensity for the case of SF from an inhomogeneously broadened medium with the assumption of a Lorentzian line shape.[35] Plots of the temporal evolution of the ensemble-averaged intensity found by evaluating Eq. (15) for various values of the gain for a fixed number $N=3.0\times10^9$ of excited atoms are given by the dashed lines in Fig. 4. Note that for low values of the gain the ensemble-averaged intensity reaches a steady-state value before much of the energy of the system has been radiated, as is characteristic of ASE. We assign a delay time to the ensemble-averaged intensity through the use of a reference intensity. We take this reference intensity to be 85% of the value of the intensity at the time at which half of the atoms have radiated. The solid line in Fig. 3(b) shows the predictions found from using Eq. (15) for the delay time of the ensemble-averaged intensity. The predictions found from using Eq. (15) are in good agreement with the results of the experiment and the numerical theory for the delay time of the ensemble-averaged intensity.

Some conceptual understanding of the distinction between SF and ASE can be obtained by studying Eq. (15) in its various limits. For $\tau\gg1$, the first term of this equation becomes approximately

$$\langle I(\tau)\rangle=\exp(4\tau^{1/2}-2\tilde{\gamma}_2\tau)/8\pi N\tau . \tag{16}$$

This equation describes a pulse of radiation which peaks at the time $\tau=4\tilde{\gamma}_2^{-2}$ and which dies out for $\tau\gg\tilde{\gamma}_2^{-1}$. For times so large that the first term has essentially died out, the second term of Eq. (15) can be estimated by formally replacing the upper limit of integration by infinity, which gives $\langle I\rangle=\tilde{\gamma}_p\exp(\tilde{T}_2)[I_0(\tilde{T}_2)-I_1(\tilde{T}_2)]/N\tilde{\gamma}_2$. For the case of interest in which $\tilde{T}_2(=\alpha L/2)\gg1$ this equation becomes

$$\langle I\rangle=\exp(\alpha L)/2\pi N\tilde{T}_2^{\text{eff}} , \tag{17}$$

where $\tilde{T}_2^{\text{eff}}=\tilde{\gamma}_p^{-1}(\alpha L/\pi)^{1/2}$ is roughly the correlation time of the emission. This result describes a steady-state regime of the emission, i.e., ASE.

The predictions of Eqs. (16) and (17) are, of course, based on the use of linearized equations that do not account for population depletion. However, one can estimate the delay time τ_D by assuming the validity of Eq. (16) and calculating the time required by some fraction (say 50%) of the stored energy to be emitted. In fact, by setting

$$\int_0^{\tau_D}I(\tau)d\tau=\tfrac{1}{2} , \tag{18}$$

with $I(\tau)$ given by Eq. (16) with $\tilde{\gamma}_2$ set equal to zero, we can obtain the standard expression for τ_D given in Eq. (3). The nature of the emission is expected to be quite different depending on whether τ_D is shorter or longer than the time (T_2^2/τ_r) required to reach the peak value of the first term in Eq. (15). If τ_D is much longer than T_2^2/τ_r, the steady-state behavior described by the second term in Eq. (15) will certainly be reached before the population is significantly depleted (since for the general case of $\tilde{\gamma}_2\neq0$ the time required to deplete the inversion will be greater than or equal to the value of τ_D as calculated above) and the emission will be characteristic of ASE. The transition from SF to this type of emission occurs approximately for $\tau_D=T_2^2/\tau_r$, that is, for $T_2=(\tau_r\tau_D)^{1/2}$, which is just the Schuurmans-Polder criterion. The value of αL corresponding to the case $T_2=(\tau_r\tau_D)^{1/2}$ is marked by an arrow in Fig. 3(b) and the value of τ_D is depicted in Fig. 3(b) by the dashed line.

V. CONCLUSIONS

In summary, we have presented a quantum-mechanical theory of cooperative emission from a homogeneously broadened collection of initially inverted atoms. Through the use of the positive P representation, we have shown how this system can be described by a set of stochastic partial differential equations. We have presented numerical solutions to this set of equations for various values of the parameters to illustrate the transition of SF into ASE. We find that predictions of this theoretical model for the average delay time of the single-realization intensities and the delay time of the ensemble-averaged intensity agree well with the values of these quantities obtained from our experiment.

ACKNOWLEDGMENTS

This work was supported by the Joint Services Optics Program and by the U.S. Army Research Office, University Research Initiative. One of the authors (J.J.M.) would like to thank the U.S. Air Force Weapons Laboratory for financial support.

APPENDIX: NUMERICAL SOLUTION OF THE EQUATIONS

Equations (10) are stochastic partial differential equations for which the Itô interpretation[37] is to be used. Consistent with Itô calculus, we solve these Eqs. (7) numerically through the use of the Cauchy-Euler method.[19] This prescription leads to the algebraic equations

$$e_{x+\Delta x,\tau}=e_{x,\tau}+\Delta x p_{x,\tau} , \tag{A1a}$$

$$p_{x,\tau+\Delta\tau}=p_{x,\tau}-\Delta\tau(\tilde{\gamma}_2 p_{x,\tau}-e_{x,\tau}n_{x,\tau}-\Gamma^p_{x,\tau}) , \tag{A1b}$$

$$n_{x,\tau+\Delta\tau}=n_{x,\tau}-\Delta\tau[\tilde{\gamma}_1(n_{x,\tau}+1)+2(p^*_{x,\tau}e_{x,\tau}+p_{x,\tau}e^*_{x,\tau})-\Gamma^n_{x,\tau}] , \tag{A1c}$$

where the stochastic source terms have the form

$$\Gamma^p_{x,\tau}=[\tilde{\gamma}_p(n_{x,\tau}+1)/2N\Delta x\Delta\tau]^{1/2}(\xi_{1,x,\tau}+i\xi_{2,x,\tau}) , \tag{A2a}$$

$$\Gamma^n_{x,\tau}=[2\tilde{\gamma}_1(n_{x,\tau}+1)/N\Delta x\Delta\tau]^{1/2}\xi_{3,x,\tau} , \tag{A2b}$$

and where the initial polarization is given by

$$p_{x,0}=(2N\Delta x)^{-1/2}(\xi_{1,x,0}+i\xi_{2,x,0}) . \tag{A3}$$

The Gaussian random variables $\xi_{i,x,\tau}$ have the correlation

$$\langle\xi_{i,x,\tau}\xi_{j,x',\tau'}\rangle=\delta_{ij}\delta_{xx'}\delta_{\tau\tau'} , \tag{A4}$$

and are calculated using the Box-Muller[42] method. Note that the variables x and τ are now taken to be discrete variables that increase stepwise in value by the amounts Δx and $\Delta\tau$, respectively. The convergence of the numerical solutions was verified by ensuring that physical quantities (such as delay time) did not change when the values of the step sizes Δx and $\Delta\tau$ were changed.

*Present address: Department of Physics, University of Oregon, Eugene, OR 97403.

[1]R. H. Dicke, Phys. Rev. **93**, 99 (1954).

[2]M. F. H. Schuurmans, Q. H. F. Vrehen, D. Polder, and H. M. Gibbs, in *Advances in Atomic and Molecular Physics,* edited by D. Bates and B. Bederson (Academic, New York, 1981), p. 167.

[3]M. Gross and S. Haroche, Phys. Rep. **93**, 301 (1982).

[4]Q. H. F. Vrehen, H. M. Gibbs, in *Dissipative Systems in Quantum Optics,* edited by R. Bonifacio (Springer-Verlag, New York, 1982), p. 111.

[5]H. M. Gibbs, Q. H. F. Vrehen, and H. M. J. Hikspoors, Phys. Rev. Lett. **39**, 547 (1977).

[6]F. P. Mattar, H. M. Gibbs, S. L. McCall, and M. S. Feld, Phys. Rev. Lett. **46**, 1123 (1981).

[7]D. J. Heinzen, J. E. Thomas, and M. S. Feld, Phys. Rev. Lett. **54**, 677 (1985).

[8]M. S. Malcuit, J. J. Maki, D. J. Simkin, and R. W. Boyd, Phys. Rev. Lett. **59**, 1189 (1987).

[9]L. Allen and G. I. Peters, Phys. Rev. A **8**, 2031 (1973).

[10]U. Ganiel, A. Hardy, G. Neumann, and D. Treves, IEEE J. Quantum Electron **QE-11**, 881 (1975).

[11]S. R. Wilk, R. W. Boyd, and K. J. Teegarden, Opt. Commun. **47**, 404 (1983).

[12]J. C. Garrison, H. Nathel, and R. Y. Chiao, J. Opt. Soc. Am. B **5**, 1528 (1988).

[13]R. J. Glauber, Phys. Rev. **131**, 2766 (1963).

[14]E. C. Sudarshan, Phys. Rev. Lett. **10**, 277 (1963).

[15]H. Haken, in *Licht und Materie,* Vol. 25/2C of *Handbuch der Physik,* edited by L. Genzel (Springer-Verlag, Berlin, 1970).

[16]W. H. Louisell, *Quantum Statistical Properties of Radiation* (Wiley, New York, 1973).

[17]P. D. Drummond and C. W. Gardiner, J. Phys. A **13**, 2353 (1980).

[18]P. D. Drummond and D. F. Walls, Phys. Rev. A **23**, 2563 (1981).

[19]C. W. Gardiner, *Handbook of Stochastic Methods* (Springer-Verlag, Berlin, 1983).

[20]P. D. Drummond and S. J. Carter, J. Opt. Soc. Am. B **4**, 1565 (1987).

[21]R. Friedberg and S. R. Hartmann, Phys. Lett. **37A**, 285 (1971).

[22]N. E. Rehler and J. H. Eberly, Phys. Rev. A **3**, 1735 (1971).

[23]D. Polder, M. F. H. Schuurmans, and Q. H. F. Vrehen, Phys. Rev. A **19**, 1192 (1979).

[24]M. F. H. Schuurmans and D. Polder, Phys. Lett. **72A**, 306 (1979).

[25]M. F. H. Schuurmans, Opt. Commun. **34**, 185 (1980).

[26]F. T. Arecchi and E. Courtens, Phys. Rev. A **2**, 1730 (1970).

[27]R. Florian, L. O. Schwan, and D. Schmid, Solid State Commun. **42**, 55 (1982); Phys. Rev. A **29**, 2709 (1984); L. O. Schwan, R. Florian, D. Schmid, E. Betz, W. Schrof, B. Walker, and H. Port, Phys. Status Solidi B **124**, 741 (1984).

[28]R. Bonifacio and L. A. Lugiato, Phys. Rev. A **11**, 1507 (1975); **12**, 587 (1975); R. Bonifacio, M. Gronchi, L. A. Lugiato, and A. M. Ricca, in *Coherence and Quantum Optics, IV,* edited by L. Mandel and E. Wolf (Plenum, New York, 1978), p. 939; in *Cooperative Effects in Matter and Radiation,* edited by C. M. Bowden, D. W. Howgate, and H. R. Robl (Plenum, New

York, 1977), p. 193.
[29]S. Haroche, in *Coherence and Quantum Optics IV,* edited by L. Mandel and E. Wolf (Plenum, New York, 1978), p. 539.
[30]C. R. Stroud, Jr., J. H. Eberly, W. L. Lama, and L. Mandel, Phys. Rev. A **5**, 1094 (1972).
[31]R. Friedberg, S. R. Hartmann, and J. T. Manassah, Phys. Lett. **40A**, 365 (1972).
[32]D. B. Fitchen, in *Physics of Color Centers,* edited by W. B. Fowler (Academic, New York, 1968), p. 293.
[33]Analysis of delay time based on an energy passage time is used by K. Rzążewski, M. G. Raymer, and R. W. Boyd, Phys. Rev. A **39**, 5785 (1989).
[34]T. Baba and K. Ikeda, J. Phys. Soc. Jpn. **50**, 217 (1981).
[35]F. Haake, J. Haus, H. King, G. Schröder, and R. Glauber, Phys. Rev. Lett. **45**, 558 (1980); Phys. Rev. A **23**, 1322 (1981).
[36]P. D. Drummond and M. G. Raymer (unpublished).
[37]N. G. van Kampen, *Stochastic Processes in Physics and Chemistry* (North-Holland, New York, 1981), p. 244.
[38]R. Glauber and F. Haake, Phys. Lett. **68A**, 29 (1978); F. Haake, H. King, G. Schröder, J. Haus, R. Glauber, and F. Hopf, Phys. Rev. Lett. **42**, 1740 (1979); F. Haake, H. King, G. Schröder, J. Haus, and R. Glauber, Phys. Rev. A **20**, 2047 (1979).
[39]Note that there is a misprint in the fourth equation of Eqs. (15) of Ref. 18 from which Eq. (8b) is found. In this equation of Ref. 18 the symbol $\gamma_\perp$ (our γ_2) should be replaced by $\gamma_\parallel$ (our γ_1).
[40]J. C. MacGillivray and M. S. Feld, Phys. Rev. A **14**, 1169 (1976).
[41]M. G. Raymer and J. Mostowski, Phys. Rev. A **24**, 1980 (1981).
[42]W. H. Press, B. P. Flannery, S. A. Teukolsky, and W. T. Vetterling, *Numerical Recipes* (Cambridge University Press, New York, 1986), p. 202.